J Mater Sci (2008) 43:7418–7425
DOI 10.1007/s10853-008-2746-3

ULTRAFINE-GRAINED MATERIALS

Precipitation hardening and grain refinement in an Al–4.2wt%Mg–1.2wt%Cu processed by ECAP

V. Vidal · Z. R. Zhang · B. Verlinden

Received: 7 March 2008 / Accepted: 20 May 2008 / Published online: 13 July 2008

Abstract The precipitation and the strength evolution during equal channel angular pressing performed at 180 °C in an Al–4.2wt% Mg–1.2wt%Cu alloy have been studied by room temperature compression tests and transmission electron microscopy. The age hardening behaviour of these AlMgCu alloys, in which the precipitation sequence involves the S-phase and its precursors, was investigated and revealed a yield strength peak after 8 days at 180 °C. The influence of the Severe Plastic Deformation on the microstructure and mechanical properties of under-aged and peak-aged samples are presented. Notably, in the under-aged sample, a gradual increase of the strength after each ECAP pass is obtained while, the peak-aged samples loose much of their strength during the first ECAP pass. TEM characterization of the microstructure before and after ECAP is presented and linked to the evolution of the mechanical properties.

Introduction

Metals with grain sizes smaller than 1 μm have received much attention in the past decade as they are characterized by an improvement of the mechanical and physical properties. These materials have been classified as ultra fine grain (UFG) materials (grain sizes in the range of 100–1,000 nm) and nanomaterials (grain size <100 nm). Since the early 1990s, a number of severe plastic deformation (SPD) methods for producing bulk UFG metals, have been developed, among which the equal channel angular extrusion or pressing (ECAE/P) appears to be one of the most promising of these processes [1, 2].

This process involves introducing large shear strain into the material by pushing it through a die that consists of two channels with the same cross-sectional shape that meet at an angle to each other. Since the cross-sections of the two channels are the same, the extruded product can be re-inserted into the entrance channel and pushed again through the die. Repeated extrusion through the ECAE/P die accumulates sufficient strain to breakdown the microstructure and produces an ultra fine grain size [3].

Several studies have demonstrated that ECAP processing can be very effective for grain refinement and production of ultra fine grain sizes in numerous Al alloys [4, 5]. However, in the case of precipitation hardenable aluminium alloys, the influence of the precipitates as well as their evolution during ECAP processing are still not clear since depending on the aluminium alloy system (and so depending on the nature of the precipitates) several features have been reported: increase or decrease of the hardness depending on the initial ageing level, precipitation and/or dissolution of the precipitates into the matrix and very significant changes in the precipitate morphology [6, 7]. Nevertheless, it is widely reported that ECAP can led to ultra fine grain size and also that rod shape precipitates are severely deformed or fragmented by the shear strain introduced during ECAP (for example $MgZn_2$ precipitates in an Al-7034 alloy [8] or θ' precipitates in an Al–1.7at.%Cu alloy [7]).

V. Vidal (✉) · B. Verlinden
Department of Materials Engineering, KUL, Kasteelpark Arenberg 44, 3001 Heverlee, Leuven, Belgium
e-mail: Vanessa.Vidal@mtm.kuleuven.be;
Vanessa.Vidal@enstimac.fr

B. Verlinden
e-mail: Bert.Verlinden@mtm.kuleuven.be

Z. R. Zhang
Department of Mechanical Engineering and Intelligent Systems, University of Electro-Communication, Chofugaoka 1-5-1, Chofu, Tokyo 182-8285, Japan

The aim of the present investigation is first to characterize the ageing behaviour of an Al–4.3 wt%Mg–1.2%Cu alloy and then to provide information on the evolution of the strength and microstructure (precipitates as well as grain size) during consecutives ECAP passes applied on under-aged and peak-aged samples. Particular care is taken to link the nature, the morphology of precipitates and the refinement of the microstructure with the evolution of the mechanical properties during the first ECAP passes.

Experimental material and procedures

The experiments were conducted on an Al–4.3wt%Mg–1.2wt%Cu alloy obtained by addition of 1.2wt%Cu into a commercial AlMg alloy (AA5182) to make this alloy precipitate hardenable. It has a chemical composition (in wt%) of 4.331%Mg–1.233%Cu–0.306%Fe–0.134%Si–0.029%Cr with as balance Al.

For the study of the ageing behaviour, samples cut from the as cast billet were slowly heated to 530 °C, homogenized for 24 h at 530 °C in an inert gas atmosphere of argon and then cooled in air. Subsequently, these samples were solution-treated for 30 min at 530 °C and water quenched in a solution containing 5vol%KOH + 5 vol%NaCl.

These as-quenched samples were artificially aged in a salt bath at 180 °C for various times (from 15 min to 32 days) and quenched. The yield strength (YS) was evaluated by means of compression tests on as-quenched and aged samples cut with the long axis parallel to the casting direction of the former ingot and with a gauge length of 9 mm and diameter of 6 mm. All compression tests were carried out at room temperature using an INSTRON 4505 machine with a constant crosshead displacement rate of 0.20 mm/min equivalent to an initial strain rate of $3.7 \times 10^{-4}\ s^{-1}$. The yield strength was determined at 0.2% true strain.

ECAP samples were cut also from the as cast billet: they consist of rods with a diameter of 11.9 mm and a length of 50 mm with the long axis parallel to the casting direction. These rods were homogenized, solution treated and quenched as previously described. Based on the experimental results from the ageing behaviour, two different types of artificial ageing in a salt bath were carried out on the as-quenched ECAP samples: 15 min at 180 °C (under-aged) and 8 days at 180 °C (peak-aged). Then ECAP was performed on these under-aged and peak-aged samples at 180 °C using route Bc (i.e. sample rotated by 90° in the same sense after each pass) in a solid die consisting of two identical channels with circular cross section intersecting at an angle $\Phi = 90°$ and with an outer arc equal to 0°. These angles lead to a strain of about 1.15 in each passage through the die. The ECAP samples were coated with a lubricant containing MoS_2 and the pressing speed was 5 mm\min. The approximate time during which the sample was in the die at 180 °C is about 35 min (time for the sample with lubricant to reach the temperature of the die + deformation + waiting time after deformation). The latter waiting time is inherent to the design of the die as the first sample is pushed out of the die by the second sample. Specimens for micro hardness (Hv) measurements and compression tests were cut from the centre of extruded rods perpendicular to the longitudinal axis. Samples for transmission electron microscope (TEM) analysis were cut, using a low saw speed, from central parts of the pressed rods in sections both parallel and perpendicular to the pressing direction. They were mechanically ground to a thickness of about 100 μm and electro polished at 15 V in a solution of 20% perchloric acid and 80% methanol at a temperature of −35 °C using a Tenupol-5 twin-jet polishing unit. The TEM observations and EDX (Energy Dispersive X-ray) analysis were performed on a Philips CM 200FEG operated at 200 kV.

Results and discussion

Characterization before ECAP: ageing curve and microstructure

The evolution of the compressive yield stress of the Al–4.3wt%Mg–1.2wt%Cu alloy as a function of the ageing time at 180 °C is shown in Fig. 1. The age hardening curve of this alloy shows different typical stages : after an initial YS increase, the curve exhibits a long plateau, or slight linear increase, which is followed by a second stage of hardening towards the peak of YS which appeared after 8 days (peak-aged sample). At the final stage of ageing, the YS decreased gradually as a result of overageing. This ageing curve is in agreement with results reported in literature for similar alloys [9–11].

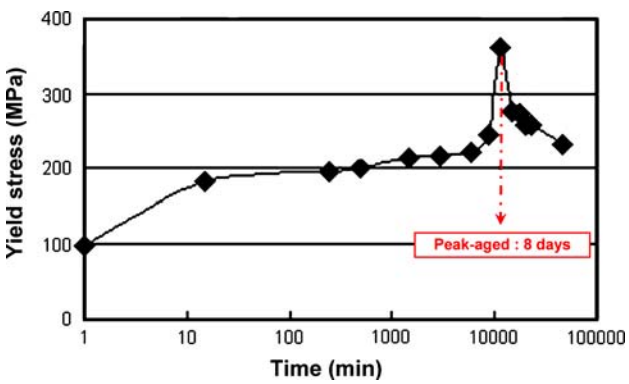

Fig. 1 Compressive yield stress of an Al–4.3wt%Mg–1.2wt%Cu alloy as a function of the ageing time at 180 °C

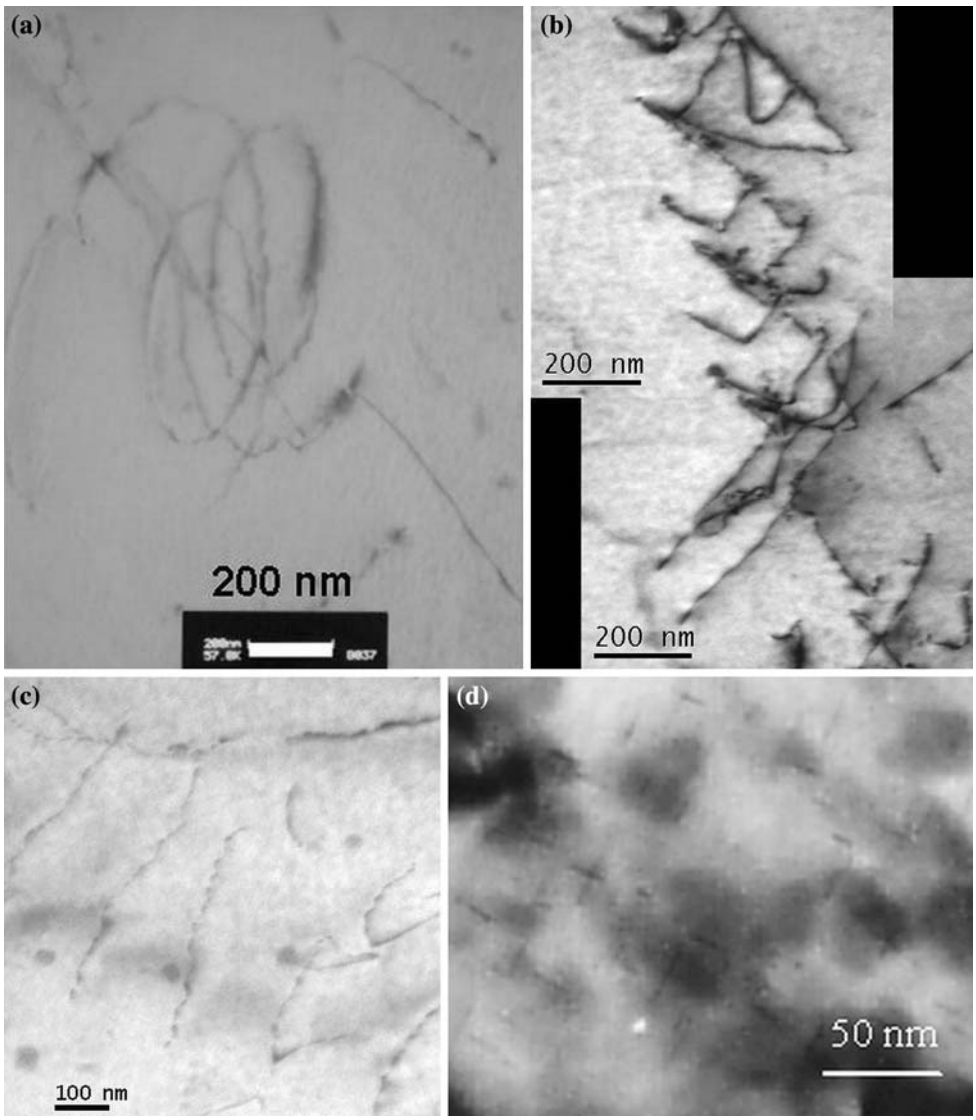

Fig. 2 Bright Field (BF) TEM micrographs of the AlMgCu alloy in under-aged conditions (**a**–**c**) after 15 min of artificial ageing at 180 °C and (**d**) 8 h at 180 °C

The precipitation hardening sequence in AlMgCu alloys having Mg:Cu mass ratios >1 has been studied by several authors [10, 12] and, even if the precise precipitation mechanisms are still under discussion, the following precipitation sequence is generally proposed: supersaturated $\alpha \rightarrow$ Cu/Mg co-clusters (or GPB zones) $\rightarrow$ S″ (or GPBII zones) $\rightarrow$ S′ $\rightarrow$ S, where GPB zones (or Cu/Mg clusters) may contribute to the initial increase of strength. S″ and S′ are two semi-coherent intermediate precursor of the equilibrium S phase (Al_2CuMg) which is not coherent with the matrix. It is further mostly accepted that S′ and S only differ in the degree of coherency. Nevertheless, as presented by Kovarik et al. [13], the origin of the rapid hardening is still not well understood and has been interpreted by either the GPB zone (even if there is no direct evidence confirming their existence), or solute cluster hardening [14] or also dislocation-solute interaction [15].

Figure 2 shows four TEM images of the AlMgCu alloys in under-aged condition (Fig. 2a–c: ageing 15 min at 180 °C and d: 8 h at 180 °C). First of all, the presence of uniform arrays of dislocations and dislocation ellipses is noticed. It appears that the dislocations are clearly pinned which may be related to the presence of very fine precipitates (GPB zones? Cu/Mg clusters?) not identifiable by conventional TEM observation. Previous publications have shown that GPB zones in AlMgCu alloys can only be detected by TEM after several hours of ageing at 180 °C [13]. After 8 h, the Cu/Mg clusters (or GPB zones) developed into a uniform distribution of fine needle-like precipitates as shown on Fig. 2d. These precipitates, elongated along specific directions of the matrix, have a length of around 30 nm and very low thickness values (order of a few nanometers). Spherical precipitates with a mean diameter of 30 nm, not responsible for the pinning of

the dislocation, are also noticed (Fig. 2c). Even if EDX measurements revealed that they correspond to Cu-riches zones, the nature of these precipitates is not so clear. The lack of strain contrast around the particles at different tilt, shows their non-coherency with the matrix. Moreover they do not interact with the dislocations, thus, it can be supposed that these spherical particles do not play a key role here. Hence, in the under-aged condition, the microstructure is most probably mainly composed of co-cluster Cu/Mg (or fine GPB zones) supposed to be responsible of the first YS increase by pinning the dislocations.

Figure 3 shows two TEM pictures of the AlMgCu alloys in peak-aged condition (8 days at 180 °C), i.e. when the YS reached a maximum value. The typical microstructure in the peak-aged condition is completely different from the one in under-aged condition. It consists of a uniform distribution of rod-shaped precipitates elongated along the $<100>_{\alpha}$ directions of the matrix and thus we can observe them either in the "horizontal" position (elongated) or "vertical" position (spherical cross section as seen on Fig. 3b). These precipitates may be the result of the growth of the fine needle-like precipitates observed after 8 h of ageing (Fig. 2d). Nevertheless, we distinguish a co-existence of two types of elongated precipitates which can be described in the order of their typical sizes.

The first type of precipitates has a length of around 100–200 nm and a thickness close to 20 nm (Fig. 3a–c). They are surrounded by a typical strain field contrast revealing their semi-coherency with the matrix. With these characteristics and based on previous studies in similar alloys [16], it is assumed that these precipitates correspond to the S′ phase. The second type of elongated precipitates, as seen on Fig. 3b, is clearly thinner. They have a length of around 50 nm and a low thickness close to 1 nm. From a few HRTEM pictures (not shown here) and Fourier Transforms (FFT) showing strikes instead of spots, it can be deduced that these thin precipitates are GPB zones. Nevertheless, due to a lack of "statistics" and not a really high quality of

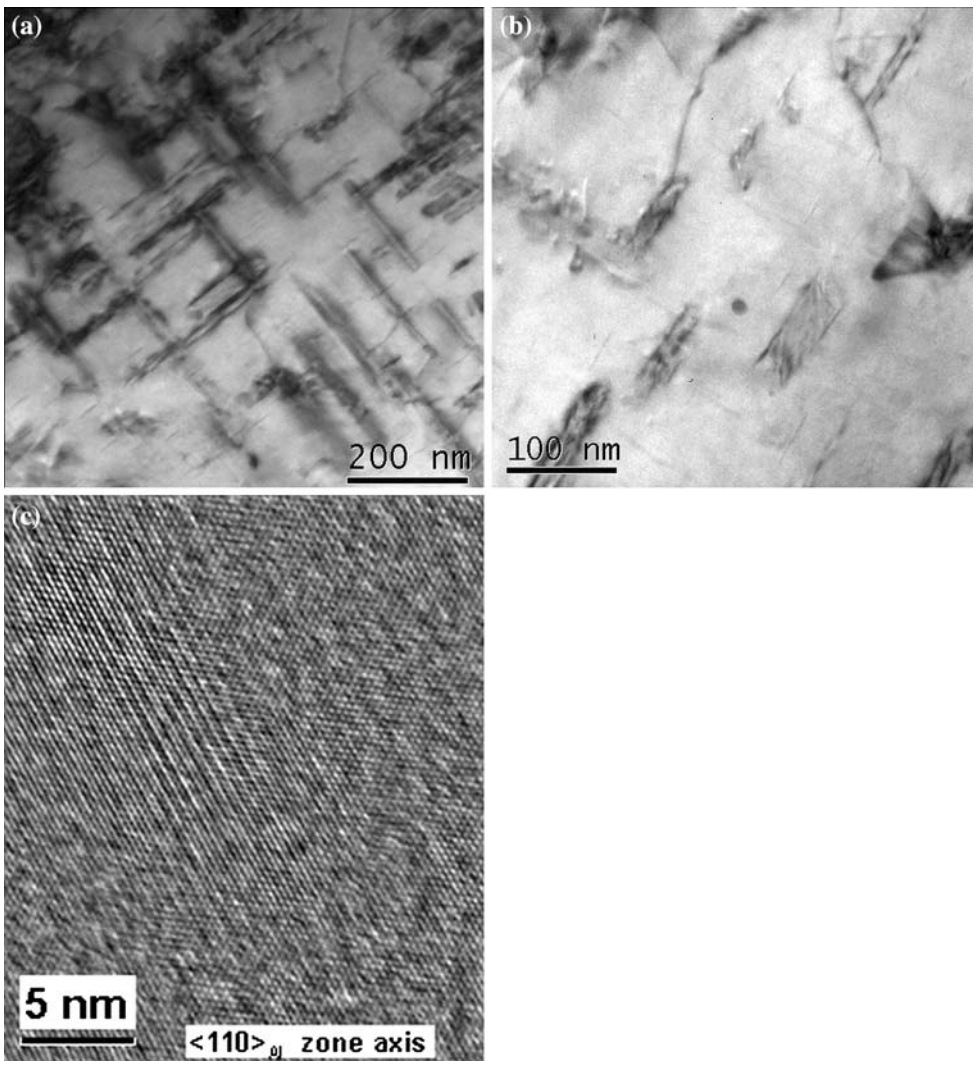

Fig. 3 BF TEM micrographs of the AlMgCu alloy after 8 days of artificial ageing at 180 °C (peak aged sample): (**a**) overview (**b**) higher magnification revealing the presence of both, fine and large elongated precipitates and (**c**) HRTEM picture showing one part of the largest precipitate (S′ phase)

the HRTEM pictures, it is difficult to conclude on the nature of these precipitates: indeed by comparing with data from the literature they could also be S″ phase (sometimes referred as a GPBII zone).

What is important here is that the peak-aged hardening is directly linked to an homogeneous and efficient distribution of two main types of elongated precipitates (both precursor of the S phase) which are semi-coherent (continuity of the lattice plane at least in one direction) with the matrix.

Characterization after ECAP: mechanical properties and microstructure evolution

Figure 4 shows the influence of the ageing treatment (under-aged and peak-aged) and ECAP processing on the yield stress of the present AlMgCu alloy. For under-aged samples (15 min at 180 °C), the yield stress increases continuously from the solid solution state till the under-ageing state after 4 ECAP passes. For peak-aged samples (8 days at 180 °C), this figure reveals an interesting feature: after the first ECAP pass, a decrease of the YS happens and then the YS slightly increases between 2 and 4 passes. In order to understand these two different behaviours occurring during the ECAP passes, and especially during the first ECAP pass, TEM observations were done on under- and peak-aged samples after 1 and 4 ECAP passes.

Figure 5 shows the microstructure in under-aged samples observed by TEM after processing by ECAP through 1 pass at low (a) and high (b) magnifications and after 4 passes (c, d). The microstructure after one pass consists of local banded dislocation arrays corresponding to deformation bands where the development of cells, subgrains and low angle grain boundaries is in progress. Indeed, in Fig. 5a and b a beginning of the microstructural refinement with a complex dislocation network and local rearrangement of the dislocations in tangles is evidenced. After 4 ECAP passes, the microstructure consists mainly of remnant elongated subgrains, the width of which being almost the same as the initial deformation band (500 nm to 1 μm), and also of equiaxed grains with an average size of approximately 200 nm. While the finer grains are almost free of dislocation, still tangled dislocations are observed in the larger remnant subgrains suggesting that the refinement is still in progress. Note that previous EBSD experiments have shown that after 4 ECAP passes at 200 °C, this type of Al alloy (in as-quenched condition) consists of 24% high angle grain boundaries (misorientation >15°) with an average (sub)grain size of 2.3 μm [11].

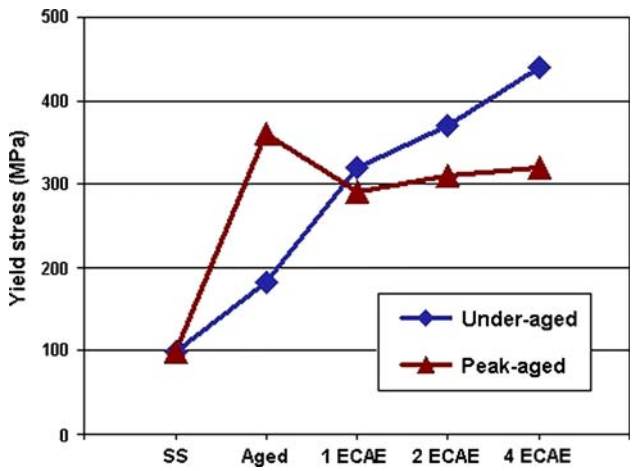

Fig. 4 Influence of "ageing treatments" and "ageing treatment + ECAP" on the yield strength of the AlMgCu alloy

Concerning the precipitate "landscape", TEM observations for studying the evolution during ECAP of the "precipitates or co-clusters" responsible of the dislocation pinning before ECAP, failed. Nevertheless, it is noticed that the amount of the spherical precipitates clearly decreases, indicating their possible dissolution into the matrix. Thus, it is reasonable to conclude that the high strength obtained after 4 ECAP passes at 180 °C originates mainly from the increase of the dislocation density (=high work hardening) during the first ECAP pass and then to the progressive grain refinement of the microstructure. Moreover the dislocation interactions with both the "co-clusters" and the elements in solid solution may contribute, to a lower extent, to the enhancement of the YS.

Contrary to the under-aged sample, in the peak-aged sample the size, distribution and nature of the precipitates play a key role to the initial high YS value. Thus, a "precipitate landscape" evolution during the successive ECAP passes may drastically influence this YS value. Figure 6 shows TEM pictures obtained in the peak-aged sample after 1 pass (a–c) and 4 passes (d).

Due to an increase of the dislocation density (complex dislocation network in Fig. 6a) and their associated strain field, it is difficult to observe easily the precipitates. Nevertheless, it appears that the length of the largest elongated precipitates becomes shorter after 1 pass and that they are distributed linearly in a rod-like configuration. This indicates that the very high stresses imposed during ECAP lead to a fragmentation of the larger rod-like precipitates: indeed in Fig. 6c the precipitates are clearly fragmented by shearing into many small pieces which morphology may tend to a spherical shape. It should be noted that the fragmentation of precipitates during ECAP was also reported in earlier studies, e.g. θ' in AlCu [7], S′ in AA2024 [17], η in Al-7034 [8] or β' in AlMgSi [18]. Moreover, it was noticed from these TEM observations that the amount of the finest precipitates tends to decrease indicating their partial dissolution.

Due to the high pressure applied during ECAP, the size, the inter-particle spacing, the shape and the amount of the

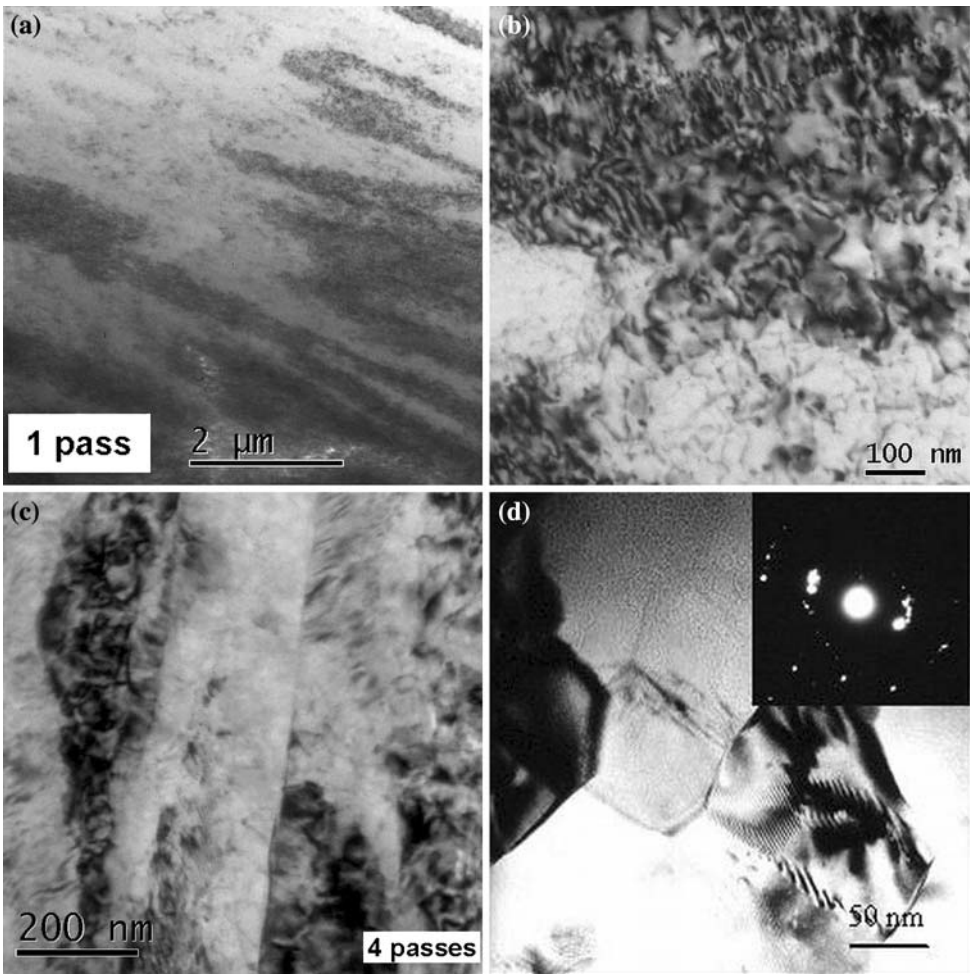

Fig. 5 TEM micrographs of under-aged AlMgCu alloy processes by ECAP at 180 °C for (**a**) 1 pass (**b**) 1 pass higher magnification (**c**, **d**) 4 passes

nano-precipitates do not longer correspond to the most efficient "microstructural configuration", responsible for the peak aged hardening. Thus, during the first ECAP pass and despite an increase of the dislocation density, it appears that the decrease of the YS is directly linked to the change in shape, size and distribution of the precipitates leading to a less efficient "precipitate landscape". After 1 pass, the fragmentation of the largest S′ precipitates added to the dissolution of the finest precipitates lead to an important loss of strengthening which cannot be compensated by the "dislocation strengthening" contribution. It should be noted here, that the loss of strength is mainly attributed to the dissolution of the finest precipitates. Nevertheless, the fragmentation of the largest semi-coherent precipitates may also contribute to this lower strength. Indeed, classical age-hardening curves of Al alloys (hardening versus precipitates size) are characterized by an increase of the strength with the coarsening of the coherent precipitates, followed by a decrease when the precipitates are too large and become non-coherent. Thus, while the fragmentation of non-coherent precipitates should normally increase the strength of the alloy, for coherent and semi-coherent precipitates (our case), a decrease of the strength should occur. Moreover, rather than being distributed homogenously into the Al matrix, the largest precipitates are, after ECAP, distributed linearly in "rod-like" configuration. Then due to this feature and to their new morphology (less elongated and more spherical), the influence of the stress field generated by these nanoprecipitates on the movement of the dislocations may be less efficient.

Nevertheless, from 2 passes on, the YS value increases again, evidencing a higher contribution of dislocations and refinement strengthening at this strain level. Finally, after 4 passes, equiaxed (sub)grains are obtained (Fig. 6d).

It is interesting to note here, that the microstructure in the over-aged condition (not shown in this article, but discussed in [19]) consists of homogeneous large rod-shaped precipitates (supposed to be the S′/S phase): it differs from the peak-aged sample by an increased size and a reduced density of the precipitates where the fine precipitates observed in the peak-aged sample may have grown and/or coarsened and thus are no longer present (there are just large precipitates). These main differences lead to a low contribution of

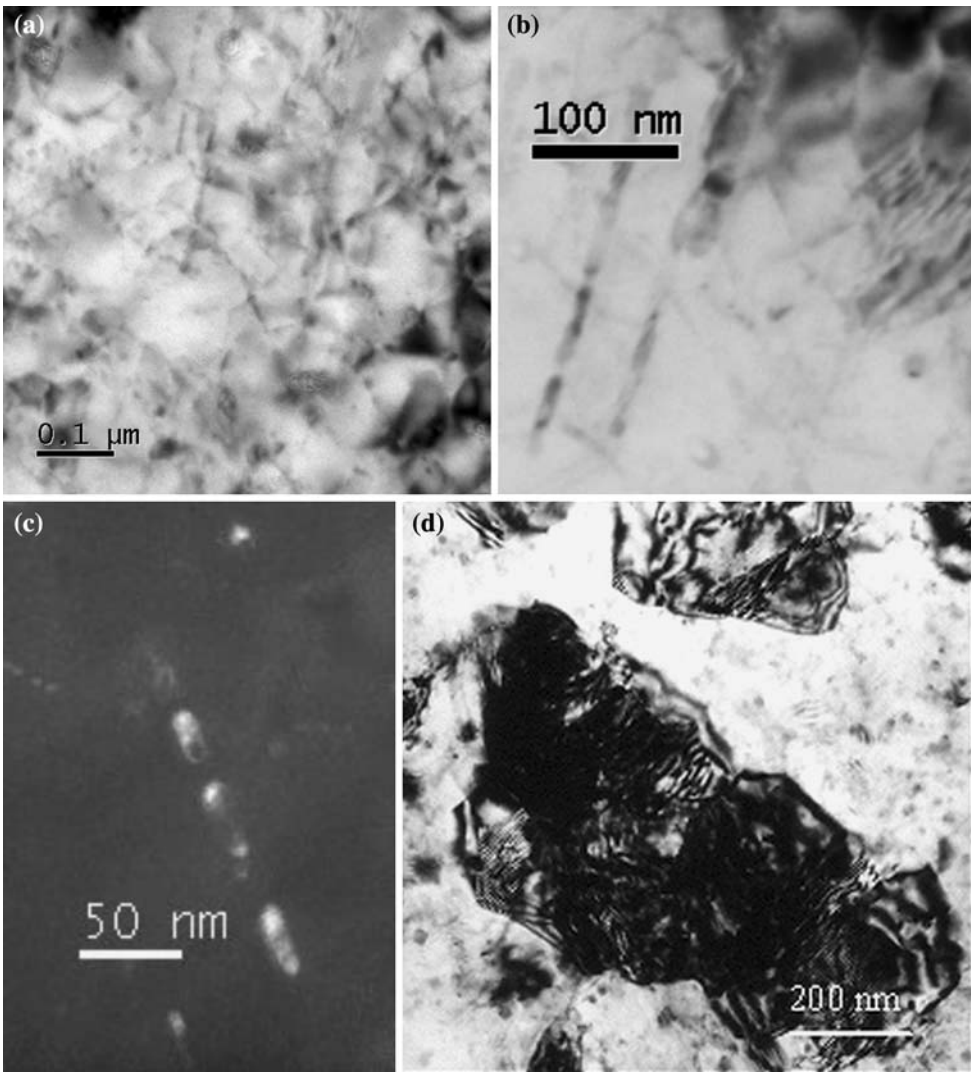

Fig. 6 TEM micrographs of the peak-aged AlMgCu alloy processes by ECAP at 180 °C for (**a–c**) 1 pass (c-dark field showing precipitate fragmentation) (**d**) 4 passes

the precipitates to the strengthening since precipitate coarsening increases the distance between precipitates, making dislocations bowing easier. Then during the ECAP passes, while the fragmentation of large precipitates occurred as in the peak-aged sample, there is no dissolution as no fine precipitates are present initially. In the same time a slight increase (and no decrease) of the YS value is observed: the "dislocation strengthening" associated to the "refinement strengthening" due to ECAP are, in over-aged samples, the main contributors to the measured YS.

This feature also evidenced that the reduction of strength during the first ECAP pass of the peak-aged sample may be attributed, to a larger extent, to the dissolution of the finest precipitates.

Conclusion

The ageing behaviour of an Al–4.3wt%Mg–1.2wt%Cu alloy was studied at 180 °C. The YS evolution during ageing is characterized by an initial increase, followed by a plateau or slight increase and a peak of strength which appears after 8 days. In the under-aged condition, the microstructure is mainly composed of (i) co-clusters of Cu/Mg (or fine GPB zones) supposed to be responsible of the first YS increase by pinning the dislocations and (ii) spherical nanoprecipitates. In the peak-aged condition, an homogeneous and efficient distribution of two main types of elongated precipitates (both, the largest and the finest one being precursor of the S phase) which are semi-coherent with the matrix are the main contributing factors to the peak of strength.

The highest strength was achieved after four ECAP passes realized at 180 °C on samples in under-aged condition. The origin of this high YS value is mainly attributed to dislocation- and grain refinement strengthening due to ECAP and also, to a lower extent, to dislocation interactions with both the "co-clusters" and the alloying elements in solid solution (due to a partial dissolution of the spherical nanoprecipitates).

On the contrary, processing by ECAP at 180 °C in the peak-aged condition led to the fracture of the large rod-shaped S′ phase precipitates and also to the partial dissolution of the finest rod-shaped precipitates. A YS decrease after the first ECAP pass is then attributed mainly to this dissolution but also to the significant precipitate fragmentation. Then, from 2 passes on the contributions of dislocation strengthening (work hardening) associated to the refinement strengthening due to ECAP, led to a YS increase.

Finally, processing by ECAP plays a dual role in this AlMgCu alloy by both refining the grain size and also significantly altering the morphology and amount of precipitates. So to obtain efficient strengthening of age hardenable aluminium alloys by ECA pressing, the complex interaction between, precipitation and grain refinement, has to be investigated carefully.

References

1. Valiev RZ, Islamgaliev RK, Alexandrov IV (2000) Prog Mater Sci 45:103. doi:10.1016/S0079-6425(99)00007-9
2. Valiev R (2004) Nat Mater 3:511. doi:10.1038/nmat1180
3. Valiev RZ, Langdon TG (2006) Prog Mater Sci 51:881. doi:10.1016/j.pmatsci.2006.02.003
4. Iwahashi Y, Horita Z, Nemoto M, Langdon TG (1998) Metall Mater Trans 29A:2503
5. Horita Z, Fujinami T, Nemoto M, Langdon TG (2001) J Mater Process Tech 117:288. doi:10.1016/S0924-0136(01)00783-X
6. Szczygiel P, Roven HJ, Reiso O (2005) Mater Sci Eng A 410:261. doi:10.1016/j.msea.2005.08.051
7. Murayama M, Horita Z, Hono K (2001) Acta Mater 49:21. doi:10.1016/S1359-6454(00)00308-6
8. Xu C, Furukawa M, Horita Z, Langdon TG (2003) Acta Mater 51:6139. doi:10.1016/S1359-6454(03)00433-6
9. Ringer SP, Hono K, Sakurai T, Polmear IJ (1997) Scripta Mater 36:517. doi:10.1016/S1359-6462(96)00415-0
10. Ratchev P, Verlinden B, De Smet P, Van Houtte P (1998) Acta Mater 46:3523. doi:10.1016/S1359-6454(98)00033-0
11. Verlinden B, Popovic M (2006) Mater Sci Forum 503–504
12. Charai A, Walther T, Alfonso C, Zahra AM, Zahra CY (2000) Acta Mater 48:2751. doi:10.1016/S1359-6454(99)00422-X
13. Kovarik L, Gouma PI, Kisielowski C, Court SA, Mills MJ (2004) Acta Mater 52:2509. doi:10.1016/j.actamat.2004.01.041
14. Ringer SP, Sakurai T, Polmear IJ (1997) Acta Mater 45:3731. doi:10.1016/S1359-6454(97)00039-6
15. Reich L, Murayama M, Hono K (1998) Acta Mater 46:6053. doi:10.1016/S1359-6454(98)00280-8
16. Ratchev P, Verlinden B, De Smet P, Van Houtte P (1999) Mater Trans JIM 40:34
17. Kang SB, Lim CY, Kim HW, Mao J (2002) Mater Sci Forum 396:1163
18. Roven HJ, Liu M, Werenskiold JC (2008) Mater Sci Eng A 483–484:54. doi:10.1016/j.msea.2006.09.142
19. Zhang Z-R, Van Houtte P, Verlinden B (2008) Int J Mater Res 3:273